THE JOURNAL OF BIOLOGICAL CHEMISTRY
Vol. 279, No. 9, Issue of February 27, pp. 7405–7412, 2004
Printed in U.S.A.

Enhanced Binding of TonB to a Ligand-loaded Outer Membrane Receptor

ROLE OF THE OLIGOMERIC STATE OF TonB IN FORMATION OF A FUNCTIONAL FhuA·TonB COMPLEX*

Received for publication, October 27, 2003, and in revised form, December 10, 2003
Published, JBC Papers in Press, December 10, 2003, DOI 10.1074/jbc.M311784200

Cezar M. Khursigara‡, Gregory De Crescenzo§, Peter D. Pawelek‡, and James W. Coulton‡¶

From the ‡Department of Microbiology and Immunology, McGill University, 3775 University Street and the §Protein-Protein Interaction Facility, Sheldon Biotechnology Center, McGill University, 3773 University Street, Montreal, Quebec H3A 2B4, Canada

The ferric hydroxymate uptake (FhuA) receptor from *Escherichia coli* facilitates transport of siderophores ferricrocin and ferrichrome and siderophore-antibiotic conjugates such as albomycin and rifamycin CGP 4832. FhuA is also the receptor for phages T5, T1, Φ80, UC-1, for colicin M and for the antimicrobial peptide microcin MccJ21. Energy for transport is provided by the cytoplasmic membrane complex TonB·ExbB·ExbD, which uses the proton motive force of the cytoplasmic membrane to transduce energy to the outer membrane. To accomplish energy transfer, TonB contacts outer membrane receptors. However, the stoichiometry of TonB·receptor complexes and their sites of interaction remain uncertain. In this study, analyses of FhuA interactions with two recombinant TonB proteins by analytical ultracentrifugation revealed that TonB forms a 2:1 complex with FhuA. The presence of the FhuA-specific ligand ferricrocin enhanced the amounts of complex but is not essential for its formation. Surface plasmon resonance experiments demonstrated that FhuA·TonB interactions are multiple and have apparent affinities in the nanomolar range. TonB also possesses two distinct binding regions: one in the C terminus of the protein, for which binding to FhuA is ferricrocin-independent, and a higher affinity region outside the C terminus, for which ferricrocin enhances interactions with FhuA. Together these experiments establish that FhuA·TonB interactions are more intricate than originally predicted, that the TonB·FhuA stoichiometry is 2:1, and that ferricrocin modulates binding of FhuA to TonB at regions outside the C-terminal domain of TonB.

Gram-negative bacteria have evolved efficient acquisition systems for the uptake of scarce nutrients. One of the most sought after nutrients is iron, an element whose bioavailability is limited at physiological conditions, because it forms insoluble ferric hydroxides. *Escherichia coli* satisfies its iron requirements by expressing high affinity receptors at its cell surface. These proteins bind and transport iron-chelating siderophores from the external milieu into the periplasm in an energy-dependent manner. One such high affinity uptake system relies upon FhuA, receptor for the hydroxamate siderophore ferricrocin (Fc).[1] FhuA also facilitates the transport of siderophore-antibiotic conjugates such as albomycin and rifamycin CGP 4832, is the receptor for phages T5, T1, Φ80, UC-1, for colicin M and for the antimicrobial peptide microcin MccJ21 (1–3). Energy for siderophore transport is provided by the cytoplasmic membrane (CM) complex TonB·ExbB·ExbD, which exploits the electrochemical potential from the proton motive force of the CM and transduces energy to the outer membrane (OM) (4).

Although many proteins involved in TonB-dependent siderophore transport have been identified and studied, the molecular mechanism of siderophore uptake from the external environment to the periplasm of the bacteria remains obscure. Evidence for conformational changes occurring in FhuA following siderophore binding was provided by differential recognition by monoclonal antibodies of ligand-free *versus* ligand-loaded receptor (5). At the atomic level, x-ray crystallographic structures of FhuA (6, 7), and the receptor FecA (8) displayed conspicuous structural changes upon ligand binding. A switch helix (residues 24–29) on the periplasmic face of FhuA unwound to a random coil, and there was a 17-Å translocation of the extreme N terminus, proximal to the Ton box of FhuA. This conformational change was proposed to be a signal reporting the ligand-loaded status of FhuA to TonB (6, 7). However, two other OM receptors, FepA and BtuB (9, 10), whose structures have been published at atomic resolution, do not contain a switch helix. The unwinding of a switch helix is therefore not a common mechanistic feature for all OM receptors.

In vivo cross-linking studies of TonB and FepA provided the first biochemical evidence of interactions between TonB and OM receptors (11). These results corroborated genetic analyses where point mutations in the Ton box of FhuA were suppressed by mutations in the *tonB* gene, suggesting a functional interaction near Gln160 of TonB (12, 13). Additional cross-linking studies demonstrated that specific ligands of the OM receptors enhance their association with TonB (14–16).

Detailed analyses of TonB·BtuB interactions by site-directed spin labeling revealed that TonB requires a specific orientation for functional contact with the Ton box. Changes in conformation in the Ton box region caused by proline substitutions abrogated transport of the ligand (17). The crystal structure of

* This work was supported by operating grants (to J. W. C.) from the Natural Sciences and Engineering Research Council of Canada and the Canadian Institutes of Health Research (CIHR). The Canada Foundation for Innovation provided infrastructure for surface plasmon resonance to the Montreal Integrated Genomics Group for Research on Infectious Pathogens and for analytical ultracentrifugation to Hôpital Ste-Justine, Montreal. Sheldon Biotechnology Center is supported by a Multi-user Maintenance Grant from CIHR. The costs of publication of this article were defrayed in part by the payment of page charges. This article must therefore be hereby marked "*advertisement*" in accordance with 18 U.S.C. Section 1734 solely to indicate this fact.

¶ To whom correspondence should be addressed. Tel.: 514-398-3929; Fax: 514-398-7052; E-mail: james.coulton@mcgill.ca.

[1] The abbreviations used are: Fc, ferricrocin; AUC, analytical ultracentrifugation; SPR, surface plasmon resonance; RU, resonance units; CM, cytoplasmic membrane; OM, outer membrane; LDAO, *N*-lauryldimethylamine oxide; CT, C-terminal; M_b, buoyant molecular mass; r.m.s.d., root mean square deviation; vbar, partial specific volume.

C-terminal TonB (residues 164–239) provided first evidence that TonB forms a dimer (18). To date, two models for TonB-OM receptor interaction have been proposed. In what has been termed the propeller model (19), two TonB monomers are intertwined, interacting with OM receptors. This model suggested that dimerized TonB undergoes rotary motion, similar to the mechanism described for the bacterial flagellar motor that is powered by MotA and MotB. ExbB and ExbD are homologous to MotA and MotB (20). An alternate model describes the shuttling of TonB between the CM and OM (19, 21). The shuttle model is supported by *in vivo* labeling experiments that demonstrate periplasmic accessibility of the extreme N terminus of TonB to the cysteine-specific marker Oregon Green 488 maleimide. According to this model, TonB in complex with ExbB and ExbD in the CM are in an unenergized conformation. ExbB·ExbD use the proton motive force to energize TonB, allowing its C-terminal portion to interact with the OM. This may cause the release of the N terminus of TonB from the CM and transfer of stored potential energy from TonB to OM receptors, thereby facilitating ligand import.

To analyze interactions between FhuA and TonB, we selected two complementary biophysical methods. Analytical ultracentrifugation (AUC) was used to determine the buoyant molecular weights and stoichiometries of two genetically engineered, soluble derivatives of TonB: a hexahistidine-tagged full-length TonB (H6.′TonB) consisting of residues 32–239 of the mature protein; and a hexahistidine-tagged C-terminal TonB (H6.′TonB (CT)), residues 155–239, both purified to homogeneity. Sedimentation velocity experiments were conducted for the two TonBs and for FhuA, either individually or as protein·protein complexes. Surface plasmon resonance (SPR) optical biosensors (Biacore) were used to derive thermodynamic parameters of the interacting proteins. Our results demonstrate that the TonB·FhuA stoichiometry is 2:1, that TonB interacts with FhuA in an Fc-independent manner, that, in addition to its C-terminal portion, the N-terminal region of TonB participates in binding to FhuA, and that Fc modulates interactions between FhuA and the N-terminal region of TonB.

EXPERIMENTAL PROCEDURES

Strains—Escherichia coli AW740 harbors plasmid pHX405 and expresses recombinant FhuA with a hexahistidine tag at position 405 (22). *E. coli* ER2566, transformed with pET28 plasmid containing H6.′TonB, was similar to the construct described by Moeck and Letellier (15) and was corrected to reflect the wild-type sequences of residues 32–239 of TonB. In addition, *E. coli* ER2566 was the host strain for pET28 into which was cloned the gene for the C terminus of TonB (residues 155–239). All plasmids were confirmed for their sequence fidelity by DNA sequencing at Sheldon Biotechnology Center, McGill University.

Protein Purification—FhuA was purified (6, 22) in *N*-lauryldimethylamine oxide (LDAO; Fluka) and detergent-exchanged using Q-Sepharose anion exchange media (Amersham Biosciences) into 100 mM HEPES (pH 7.4), 150 mM NaCl, 0.1% Tween 20 (Calbiochem), henceforth designated Biacore running buffer. H6.′TonB and H6.′TonB (CT) were purified using Ni^{2+}-nitrilotriacetic acid Superflow resin (Qiagen) followed by cation exchange on SP-Sepharose (Amersham Biosciences). Prior to SPR experiments, each TonB protein was dialyzed into Biacore running buffer. To remove the hexahistidine tag, H6.′TonB was incubated with thrombin protease (Amersham Biosciences): 1 unit of protease per mg of H6.′TonB. After 3 h at ambient temperature, the reaction mixture was applied to a Ni^{2+}-nitrilotriacetic acid column, capturing uncleaved H6.′TonB; the flow-through was applied to an SP-Sepharose column. Eluted protein was assayed by Western blotting with an anti-His6 monoclonal antibody (Cedarlane Laboratories Limited, Mississauga, Ontario, Canada) for the absence of the hexahistidine tag. TonB-reactive protein was confirmed by a cross-reactive monoclonal antibody that was raised against *Trypanosoma brucei* procyclin (CLP001A, Cedarlane) and that recognizes the proline-glutamic acid repeat portion of TonB protein. Protein concentrations were determined using the protein dye binding assay (Bio-Rad) and BCA assay (Pierce).

Analytical Ultracentrifugation—Samples were prepared for AUC by extensive dialysis against an AUC buffer: 100 mM HEPES (pH 8.0), 150 mM NaCl. In some experiments, AUC buffer was supplemented with either LDAO at 0.3% or *n*-octyltetraoxyethylene (C8E4; Bachem) at 0.4%. Protein concentrations were adjusted between 0.3 and 0.9 mg/ml. Ligand-loaded receptor was prepared by mixing Fc and FhuA in a 10:1 molar ratio, 30 min at room temperature. Excess Fc was removed by dialysis against AUC buffer using a Spectrapor dialysis membrane (POR-6, 25-kDa cutoff).

Sedimentation velocity experiments were performed on all protein samples using a Beckman XL-I Analytical Ultracentrifuge. The sample and the reference sectors of 1.2-cm path length double-sector ultracentrifuge cells were filled with 400 μl of protein and AUC buffer, respectively. All sedimentation velocity runs were performed at 40,000 rpm, with absorbance scans monitored at 280 nm in 10-min intervals over a total spin time of 4 h at 24.6 °C. Protein complexes were formed immediately prior to each spin by mixing H6.′TonB:FhuA at 1:1 and at 2:1 molar ratios, or by mixing H6.′TonB (CT):FhuA at 4:1 and at 8:1 molar ratios. In both cases, H6.′TonB and H6.′TonB (CT) were varied relative to a fixed concentration of FhuA or FhuA plus Fc.

Analysis of AUC Data—Sedimentation velocity data were analyzed by the computer program SEDFIT (23). Initial sedimentation profiles were obtained by fitting the data to the Continuous c(S) Model. Global frictional ratios determined by c(S) analysis were allowed to float to convergence. Buoyant molecular weight (M_b) and final s values were determined using the discrete non-interacting species model of SEDFIT. In sedimentation experiments involving LDAO, the detergent was modeled as a known sedimenting species with an s value of −0.1 and a micellar buoyant molecular mass of 2700 Da. Sedimentation coefficients of uncomplexed FhuA, H6.′TonB, and H6.′TonB (CT) were initially estimated from c(S) analyses and then refined by direct fitting to the Lamm equation using the non-interacting discrete species model of SEDFIT. Initial M_b values were obtained from the known molecular weights of each protein. Both s and M_b were allowed to float to convergence using the non-linear regression algorithms of SEDFIT.

Sedimentation velocity data of mixtures of FhuA plus H6.′TonB and FhuA plus H6.′TonB (CT) were fit to the discrete non-interacting species model using constrained analysis. From spins of the individual species, initial sedimentation parameters (s and M_b) of uncomplexed components ($s1$ and $s2$) were entered. The initial sedimentation parameters of predicted complexes ($s3$) were input based on the predicted M_b as integral additions of the M_b values of $s1$ and $s2$; initial sedimentation coefficients of $s3$ were estimated from c(S) analyses. The sedimentation parameters of $s3$ were then floated to convergence, whereas $s1$ and $s2$ parameters remained constrained. Fits to the model were evaluated on the basis of the distribution of residuals and r.m.s.d. errors. Optimization of the fits was performed by varying stoichiometric combinations of $s1$, $s2$, and $s3$ and repeating the constrained analyses until random distributions of residuals and minimal r.m.s.d. errors were obtained. As an unbiased test, data from mixtures of FhuA plus H6.′TonB and FhuA plus H6.′TonB (CT) were fit to the non-interacting discrete species model, assuming the presence of species with sedimentation parameters equivalent to uncomplexed $s1$ and $s2$. The r.m.s.d. errors and residuals were compared with those obtained from optimized fits in which the presence of $s3$ was modeled.

Immobilization of Recombinant TonB Proteins on Biacore Sensor Chips—Several sensor chip surfaces were assessed for binding of TonB proteins and for their regeneration, including CM4 (formerly B1), CM5, nitrilotriacetic acid (NTA), C1, and F1. Optimally, solutions of H6.′TonB (150 nM) and H6.′TonB (CT) (1.8 μM) in 10 mM acetate buffer (pH 5.5) were used to covalently immobilize the proteins on CM4 sensor chips using amine coupling procedures via *N*-hydroxysuccinimide/*N*-ethyl-*N*-(3-dimethylaminopropyl)carbodiimide hydrochloride; deactivation was accomplished with ethanolamine (24). To prepare control surfaces, activation and deactivation procedures were performed in the absence of TonB proteins.

Preliminary and Steady-state Assays by SPR—SPR measurements were performed using a Biacore 2000 and a Biacore 3000 (Biacore AB) and were carried out in triplicate at 25 °C. The data collection rate was set to 10 Hz. Biacore running buffer was used to dilute FhuA. Steady-state experiments were conducted with a flow rate of 5 μl/min. To reach steady-state equilibrium, the injection time was 1200 s followed by injections of buffer for 240 s. Regeneration was achieved by three pulses (1 min) of 5 mM NaOH, 0.1% Tween 20, and a subsequent EXTRACLEAN procedure.

Biacore Data Preparation and Analysis—Data were prepared using the double referencing method (25). For global analysis, the sensorgrams were transformed to concentration units using the molecular

TABLE I
Sedimentation velocity parameters from uncomplexed FhuA, H6.′TonB, and H6.′TonB (CT)

Protein	Φ[a]	M_b[b]	M_r[c]	M_{seq}[d]	*s*	r.m.s.d.[e]	f/f_o[f]
	ml/g		*Da*				
FhuA	0.775	18,440	81,955	80,000	3.50	0.0052	1.76
FhuA plus Fc	0.775	18,430	81,911	80,000	3.60	0.0061	1.76
H6.′TonB	0.719	6,989	27,430	24,900	1.40	0.0036	2.39
H6.′TonB (CT)	0.714	6,800	23,090	11,903	1.62	0.0035	1.96

[a] $\Phi = (1 - M_b/M_{seq})/r$.
[b] Buoyant molecular weight determined from fit to a non-interacting discrete species model.
[c] $M_r = M_b/(1 - \Phi)$.
[d] M_{seq} = molecular weight calculated from primary amino acid sequence.
[e] r.m.s.d. = least squares error of the fit to the non-interacting discrete species model.
[f] f/f_o = frictional ratio.

TABLE II
Sedimentation velocity parameters of FhuA plus H6.′TonB and FhuA plus H6.′TonB (CT) complexes determined by fits to a non-interacting discrete species model

FhuA and TonB variants were mixed in the molar ratios indicated, in the absence or presence of ferricrocin. *s*1, M_b1 = FhuA; *s*2, M_b2 = H6.′TonB (CT) or H6.′TonB; *s*3, M_b3, M_r3 = complex. For definitions of M_b, M_r, and r.m.s.d. see legend to Table I.

FhuA	H6.′TonB	H6.′TonB (CT)	Fc	*s*1	M_b1	*s*2	M_b2	*s*3	M_b3	Φ_{avg}[a]	M_r3	*s*1/*s*2/*s*3	r.m.s.d
					Da		*Da*		*Da*	*ml/g*	*Da*	% c_{tot}	
1		4	−	(3.50)[b]	(18,440)	(1.62)	(6,800)	4.47	24,177	0.761	101,158	55/18/27	0.0057
1		8	−	(3.50)	(18,440)	(1.62)	(6,800)	4.53	25,336	0.761	106,008	29/31/33	0.0049
1		4	+	(3.60)	(18,430)	(1.62)	(6,800)	4.69	24,099	0.761	100,832	38/08/40	0.0051
1		8	+	(3.60)	(18,430)	(1.62)	(6,800)	4.44	25,250	0.761	105,648	37/21/42	0.0064
1	1		−	(3.50)	(18,440)	(1.40)	(6,989)	3.24	33,403	0.762	140,348	71/05/15	0.0080
1	2		−	(3.50)	(18,440)	(1.40)	(6,989)	3.27	31,736	0.762	133,344	66/17/17	0.0057
1	1		+	−	−	1.90	(13,978)	3.53	31,201	0.762	131,096	00/10/52	0.0045
1	2		+	−	−	1.90	(13,978)	3.42	31,298	0.762	131,504	00/20/50	0.0058

[a] Φ_{avg} = weight-averaged apparent vbar of complex.
[b] Constrained parameters are indicated by *parentheses*.

weights of injected proteins. All curves were reduced to 700 evenly spaced sampling points. For each set of individual curves corresponding to injections of various concentrations of FhuA over the same surface, global fitting was carried out using a simple Langmuirian model in the SP*Revolution* software package of De Crescenzo and colleagues (26, 27). For steady-state analysis, the apparent thermodynamic dissociation constants were determined by plotting the control corrected plateau value (R_{eq}) *versus* the injected concentration of FhuA. In the case of H6.′TonB, the K_d values were derived by fitting the experimental R_{eq} values to a model of two independent population interactions,

$$R_{eq} = R_{max1} \times (C/(C + K_{d1})) + R_{max2} \times (C/(C + K_{d2})) \quad \text{(Eq. 1)}$$

where C corresponds to the injected FhuA concentration, R_{max1} and R_{max2} correspond to the maximal amount of FhuA that can be bound to each active H6.′TonB population, and K_{d1} and K_{d2} to their respective thermodynamic dissociation constants. Alternatively for H6.′TonB (CT), the experimental data were adequately fit with a simple interaction model in Equation 2 as follows.

$$R_{eq} = R_{max} \times (C/(C + K_d)) \quad \text{(Eq. 2)}$$

The fitting procedure was performed in Microsoft Excel by non-linear regression with R_{max} values and K_d values as floating parameters.

RESULTS

Analytical Ultracentrifugation—Sedimentation velocity experiments on FhuA, H6.′TonB, and H6.′TonB (CT), individually and in complex, were performed in buffers containing the neutrally buoyant detergent C8E4 such that actual molecular weight values of the protein components could be determined. In advance of determining the stoichiometry of FhuA·TonB complexes, sedimentation parameters of the individual uncomplexed species were determined and used as prior knowledge in the analysis of sedimenting complexes. To obtain the best M_r estimates of the sedimenting species, apparent vbar (Φ) values were determined from the known molecular weights of each protein, along with the buoyant molecular weights (M_b) determined by fitting to the non-interacting discrete species model of SEDFIT. As observed by Boulanger *et al.* (28), their experimentally determined vbar of FhuA (0.776 ml/g) is significantly different from the value predicted from the amino acid sequence of the protein (29). Similarly, using the known M_r of FhuA and the experimental M_b, we determine a Φ of 0.775 ml/g (Table I), in contrast to the sequence-predicted value of 0.735. The Φ values were also determined for H6.′TonB and H6.′TonB (CT), and these values (0.719 and 0.714 ml/g; Table I) also differ from vbars predicted from amino acid sequences (0.740 and 0.730 ml/g, respectively). The fits of the sedimentation velocity data of uncomplexed species to the non-interacting discrete species model were in all cases excellent with random distributions of residuals and least-squares (r.m.s.d.) errors of fit equal to or less than 0.0061.

Given these Φ values, FhuA sedimented as a monomeric protein with a molecular mass of ~80,000 Da; the presence of bound Fc resulted in a small yet reproducible increase in the sedimentation coefficient from 3.50 to 3.60 *s*, possibly due to structural rearrangements in the protein upon binding to ligand as has been observed in many of the crystal structures of bacterial OM receptors (6–9, 30). H6.′TonB sedimented as a monomer in C8E4-containing AUC buffer with a M_r of 27,430. H6.′TonB (CT) sedimented as a dimer with a M_r of 23,090 (Table I). Using the same data sets, analyses modeling the presence of additional oligomeric states of either TonB species resulted in extremely poor fits to the data (data not shown). Of the three proteins analyzed, c(S) analysis indicates that H6.′TonB has the highest frictional ratio: f/f_o = 2.39. This is consistent with H6.′TonB having an extended conformation in solution. H6.′TonB (CT) has a lower frictional ratio (f/f_o = 1.96), because it is a truncated form of H6.′TonB; furthermore, H6.′TonB (CT) is dimeric, resulting in the protein having a globular shape as compared with the more extended H6.′TonB.

FhuA and the two TonB species were then mixed together for sedimentation velocity ultracentrifugation and were analyzed for the formation of complexes: FhuA plus H6.′TonB (CT) and FhuA plus H6.′TonB, both in the absence and presence of Fc. Sedimentation data were analyzed by first fitting to a contin-

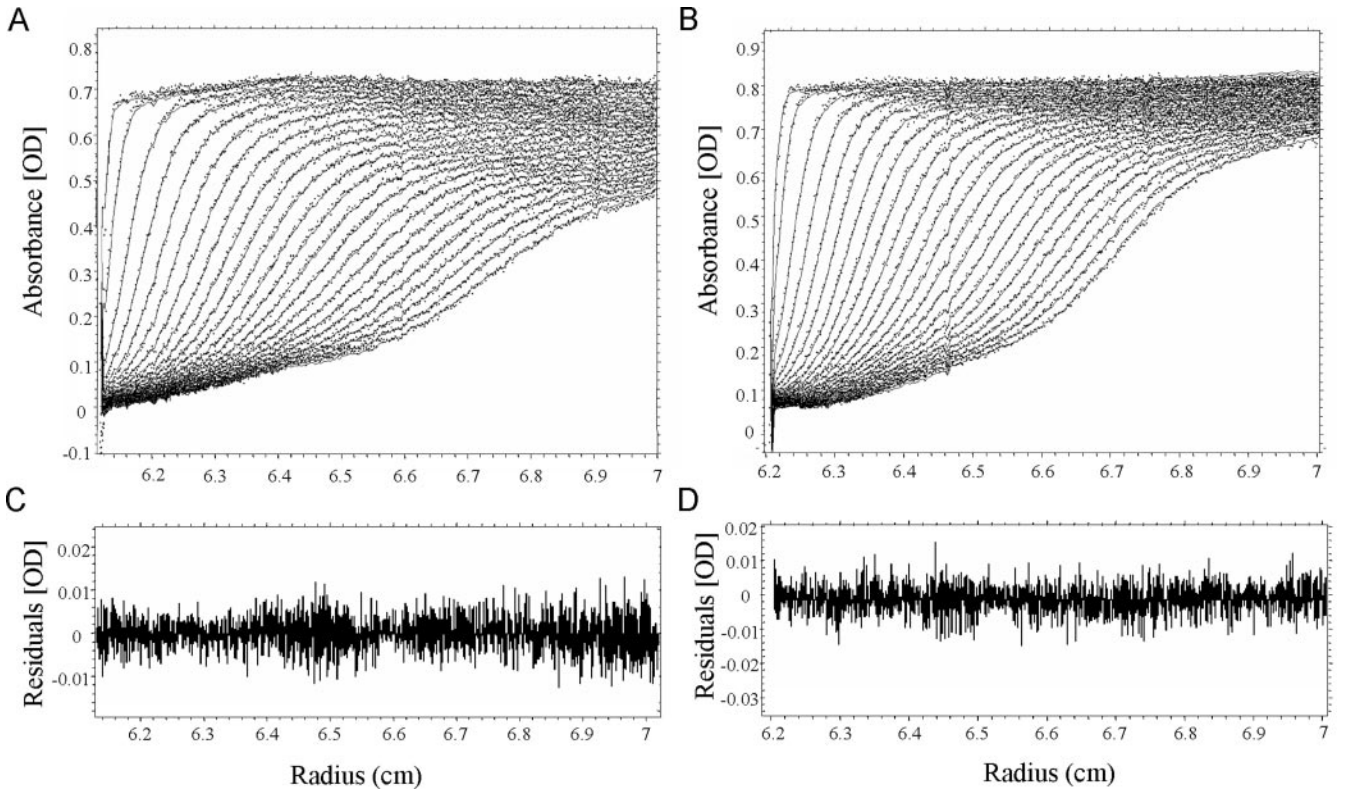

FIG. 1. **Sedimentation velocity analysis of FhuA plus Fc plus H6.′TonB (CT) and FhuA plus Fc plus H6.′TonB mixtures.** SEDFIT discrete non-interacting species model fit to 24 scans of sedimentation velocity absorbance data. *Panel A*: FhuA plus Fc:H6.′TonB (CT) at 1:4 molar ratio; *panel B*: FhuA plus Fc:H6.′TonB at 1:2 molar ratio. Model parameters (s, M_b, % c_{tot}) for each sedimenting species are identical to those used in Table II. *Dots* represent individual data points; *solid lines* represent fits of the model to the data. *Irregularities in solid lines* are the result of the noise reduction algorithms of SEDFIT. *Panel C* represents the residuals to the fit of the discrete non-interacting species model shown in *panel A*. *Panel D* represents the residuals to the fit of the discrete non-interacting species model shown in *panel B*. In *panels C* and *D*, residuals are shown for every sixth scan (scans 6, 12, 18, and 24) for each dataset.

TABLE III
Detergent effects on the sedimentation behavior of H6.′TonB and H6.′TonB (CT)
For definitions of M_b, f/f_o, and r.m.s.d. see legend to Table I.

Detergent	H6.′TonB				H6.′TonB (CT)			
	M_b	s	r.m.s.d.	f/f_o	M_b	s	r.m.s.d.	f/f_o
	Da				*Da*			
No detergent	6,951	1.56	0.0052	2.39	6,675	1.82	0.0035	1.88
C8E4	6,989	1.40	0.0036	2.20	6,800	1.62	0.0035	1.96
LDAO	5,913	1.56	0.0049	1.94	6,414	1.62	0.0035	1.74
Tween 20	11,358	1.48	0.0055	2.79				

uous c(S) model to obtain initial sedimentation parameters. This was followed (Table II) by direct fitting to the Lamm equation by a non-interacting discrete species model using the c(S)-derived sedimentation parameters and known molecular weights of individual proteins as prior knowledge (Table I). Refinement of c(S)-derived sedimentation parameters by the non-interacting species model resulted in converged s values similar to those obtained from the c(S) analysis, indicating a good correlation between the two models. However, unlike c(S) analysis, which employs a global frictional coefficient, the non-interacting species model resolves proteins of different diffusion coefficients, allowing for the calculation of buoyant molecular weight (M_b) for each sedimenting species. In the context of AUC, the term "non-interacting species" refers to sedimenting species that do not reversibly interact over the time frame of the experiment and can include stable protein complexes. In our case, a complex of FhuA and H6.′TonB (CT) or of FhuA and H6.′TonB is considered "non-interacting" if it is observed to sediment as a single species with a molecular weight that is additive of the uncomplexed components and with a sedimentation coefficient that does not significantly change as the ratio of the uncomplexed components is varied.

Experiments were performed with FhuA (−/+ Fc) mixed with either TonB species such that immediately prior to each centrifugation, proteins were combined at selected molar ratios of FhuA:H6.′TonB (CT) (monomer) = 1:4 and 1:8, or FhuA:H6.′TonB (monomer) = 1:1 and 1:2. Sedimentation velocity ultracentrifugation of these mixtures resulted in a combination of complexed species and uncomplexed species, which could be resolved by analysis of the sedimentation boundaries over the time course of the experiment. Sedimentation velocity data of both FhuA plus H6.′TonB (CT) and FhuA plus H6.′TonB mixtures fit well to the discrete non-interacting species model (Table II and Fig. 1, *A–D*). In addition to observing sedimenting species corresponding to uncomplexed FhuA ($s1$) and H6.′TonB (CT) or H6.′TonB ($s2$), a third sedimenting species ($s3$) corresponding to FhuA·TonB complex was always observed in the absence and presence of Fc. Modeling interactions without $s3$ led to dramatically poorer fits with highly non-random distributions of residuals (data not shown). The FhuA plus H6.′TonB

(CT) complex (*s*3) sedimented at ~4.5 *s*, a value significantly higher than that of uncomplexed FhuA (*s*1; 3.50 *s*). Uncomplexed dimeric H6.′TonB (CT) (*s*2) was also detected. In the absence of Fc, the abundance of *s*3 was increased significantly as the FhuA:H6.′TonB (CT) ratio increased from 1:4 to 1:8. Upon addition of Fc, a limiting amount of complex appeared to be formed at 1:4, suggesting that, although Fc is not necessary for complexation, it slightly enhanced the binding of H6.′TonB (CT) and FhuA. However, even at a FhuA:H6.′TonB (CT) ratio of 1:8, a significant proportion (37%) of FhuA remained uncomplexed in the presence of Fc (Table II).

Mixtures of FhuA plus H6.′TonB exhibited significantly different sedimentation behavior than FhuA plus H6.′TonB (CT). A sedimenting species corresponding to FhuA plus H6.′TonB complex (*s*3) was observed between 3.24 *s* and 3.53 *s*. This species was distinct from uncomplexed FhuA, having a M_b additive of uncomplexed FhuA and two molecules of H6.′TonB. Furthermore, the oligomeric state of uncomplexed H6.′TonB (*s*2) changed in the presence of Fc, resulting in a transition from monomer to dimer. Unlike the FhuA plus H6.′TonB (CT) mixtures, the addition of Fc resulted in complete disappearance of uncomplexed FhuA (*s*1), suggesting that almost all of the OM receptor in the ligand-bound state interacts with H6.′TonB. In most cases, the absorbances of *s*1, *s*2, and *s*3 accounted for at least 90% of observed c_{tot}. However, for FhuA plus Fc plus H6.′TonB mixtures (Table II, *lines 7–8*), a fourth sedimenting species was observed at ~4.0 *s* with an M_b of ~14,000 Da. This species was found to account for ~30% of c_{tot}. We previously observed a minor (<10% c_{tot}) sedimenting species at 3.6 *s* having a M_b equivalent to monomeric TonB in uncomplexed H6.′TonB solutions, likely representing an alternate conformation of H6.′TonB (data not shown). Given the presence of dimeric H6.′TonB at ~1.90 *s* in FhuA plus Fc plus H6.′TonB mixtures, it is consistent that the species at ~4.0 *s* would correspond to a dimeric form of the alternate conformation observed in uncomplexed H6.′TonB solutions.

In the case of FhuA plus H6.′TonB (CT) mixtures, the M_b of the complexes (Table II; M_b3 *lines 1–4*) is the sum of the uncomplexed species in each experiment (Table II; M_b1 and M_b2 *lines 1–4*). This reflects the binding of a H6.′TonB (CT) dimer to a FhuA monomer. This additivity is also observed for FhuA plus H6.′TonB in the presence of Fc. In the absence of Fc, however, some FhuA remains monomeric in solution while the remainder forms a 1:2 complex with H6.′TonB. A weight-averaged Φ value was determined for FhuA plus H6.′TonB and FhuA plus H6.′TonB (CT) complexes using the Φ values for the individual components and the theoretical molecular weight of the complex given a predicted FhuA:TonB stoichiometry of 1:2. In all cases, M_r values of complex determined in this manner reflect the predicted molecular weights of 1:2 FhuA·TonB complexes.

The effect of detergent interaction with the two TonB proteins was also examined. Sedimentation behavior of H6.′TonB and H6.′TonB (CT) in the presence of C8E4 or LDAO or Tween 20 revealed significant changes in M_b and *s* parameters (Table III). The M_b of both TonB proteins slightly decreased (1.40 *s*) in the presence of LDAO due to the floatation effect of the detergent, whereas the M_b of H6.′TonB increased significantly in the presence of Tween 20, reflecting the higher density of this detergent. The detergent C8E4 does not affect the M_b of either H6.′TonB or H6.′TonB (CT), because this detergent has a neutral buoyancy in aqueous solution. However, the sedimentation coefficients of both TonB proteins decreased in the presence of C8E4, suggesting that the detergent bound to these proteins and resulted in subtle changes to their overall shape, reflected by changes to the frictional coefficients. From these data, it is clear that all three detergents bound to H6.′TonB and that C8E4 and LDAO bound to H6.′TonB (CT).

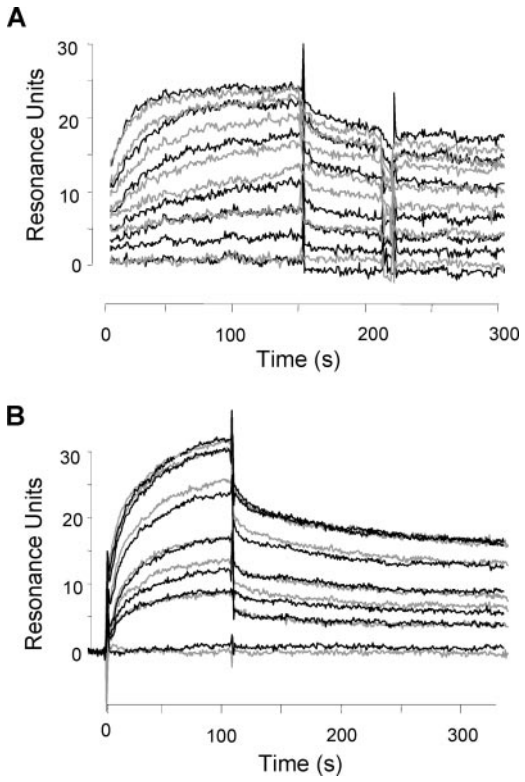

FIG. 2. **Effects of Fc on FhuA interactions with H6.′TonB and H6.′TonB (CT).** Control corrected sensorgrams corresponding to injections of FhuA (12.5–400 nM) over 35 RU of H6.′TonB (*A*) and injections of FhuA (25–400 nM) over 120 RU of H6.′TonB (CT) (*B*), in the absence (*gray*) and presence (*black*) of Fc. Experiments were performed at 25 °C at a flow rate of 100 μl/min.

Detection of FhuA·TonB Interactions by SPR—To determine the relative contribution of different portions of the TonB molecule when binding to FhuA, experiments were conducted on SPR-based biosensors, Biacore 2000 and Biacore 3000. In a typical SPR experiment, one of the binding partners (the ligand) is immobilized and the other interactant (the analyte) is injected in solution over the sensor chip surface. The resulting interaction between the ligand and the analyte is recorded in resonance units (RU), which are directly proportional to the mass accumulation on the surface. The first step in designing a Biacore experiment is to determine which interactant is to be coupled to the surface. Injections of H6.′TonB, and H6.′TonB (CT), both at 100 nM, over a control surface indicated that the two TonB proteins interacted non-specifically with the CM4 carboxymethylated dextran surface. In contrast, FhuA at the same concentration did not display nonspecific interaction. Thus the two TonB proteins were chosen to immobilize as ligand and FhuA as the detergent-solubilized analyte.

Preliminary experiments were conducted on the Biacore 2000 by coupling 35 RU of H6.′TonB. FhuA (12.5–400 nM) was preincubated with Fc (20 μM), a 50-fold excess of Fc at the highest concentration of FhuA. Injections at a flow rate of 100 μl/min resulted in significant binding when compared with a control surface. After regenerating the surface of immobilized H6.′TonB, FhuA that had not been preincubated with Fc was injected at matching concentrations; similar amounts of interacting FhuA were observed (Fig. 2*A*). These results are in contrast to reported observations that Fc enhances FhuA·TonB interactions (14, 15). To determine whether trace amounts of Fc in the Biacore 2000 system were contaminating the FhuA injections, we decided to further study the FhuA·TonB interac-

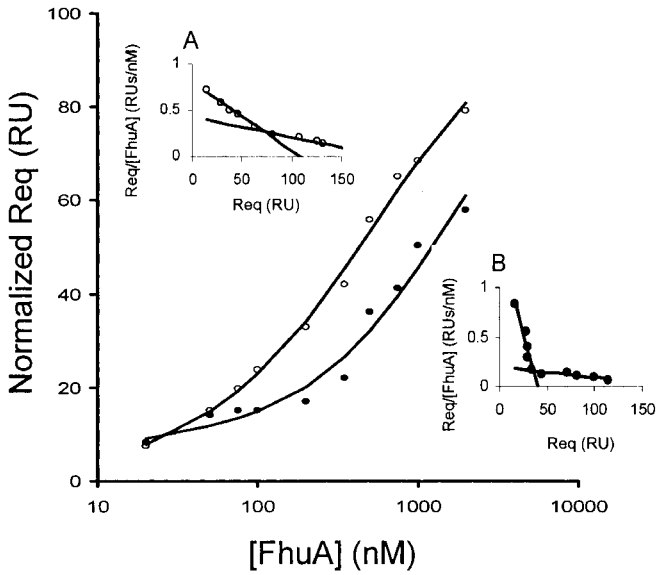

FIG. 3. **Steady-state analysis of FhuA·H6.′TonB interaction.** Normalized FhuA concentration-dependent variation of control corrected plateau resonance unit (*Req*) when injecting FhuA (ranging from 20 to 2000 nM) over two immobilized H6.′TonB surfaces. *Open* and *closed symbols* correspond to the injections performed in the absence or presence of Fc, respectively. *Solid lines* correspond to the fit when using a model that assumes the presence of two H6.′TonB populations at the biosensor surface (see "Experimental Procedures"). *Insets* correspond to Scatchard representations of the data in the absence (*inset A*) and in the presence (*inset B*) of Fc.

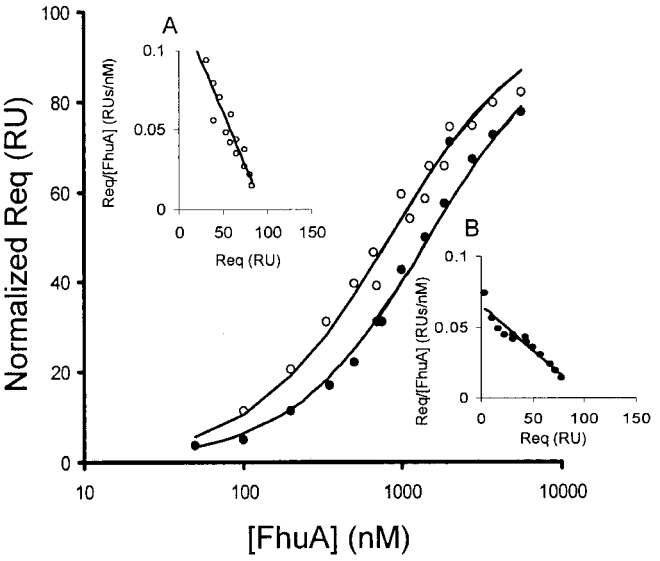

FIG. 4. **Steady-state analysis of FhuA·H6.′TonB (CT) interaction.** Normalized FhuA concentration-dependent variation of control corrected plateau resonance unit (*Req*) when injecting FhuA (ranging from 50 to 5600 nM) over three immobilized H6.′TonB (CT) surfaces. *Open* and *closed symbols* correspond to the injections performed in the absence and presence of Fc, respectively. *Solid lines* correspond to the fit when using a model assuming the presence of a single population of H6.′TonB (CT) at the biosensor surface (see "Experimental Procedures"). *Insets* correspond to a Scatchard representation of the data in the absence (*inset A*) and in the presence (*inset B*) of Fc.

TABLE IV
Thermodynamic constants from steady-state analysis of FhuA (−/+ Fc) interacting with H6.′TonB and H6.′TonB (CT)

		Low affinity population		High affinity population	
		R_{max}	K_d	R_{max}	K_d
		RU	*nM*	*RU*	*nM*
H6.′TonB	−Fc	166.5	563.5	26.2	36.5
	+Fc	179.0	1530.0	20.0	5.3
H6.′TonB (CT)	−Fc	241.0	842.0		
	+Fc	296.0	1490.0		

tion in the absence of Fc using a Biacore 3000, which had previously not been exposed to Fc. This resulted in similar responses, thus confirming the interaction between FhuA and H6.′TonB in the absence of Fc. To ensure that the interactions were specific to the TonB portion of the recombinant H6.′TonB protein and not influenced by the hexahistidine tag incorporated by the pET28 vector, equivalent amounts (30 RU) of thrombin-cleaved H6.′TonB were coupled to the sensor chip surface. Interactions with FhuA (−/+ Fc) gave similar responses as above (data not shown). The resulting sets of control-corrected sensorgrams were globally fit using a simple kinetic model. Deviations from the simple model were observed in the absence or presence of Fc as judged by the non-random distribution of the residuals (S.D. = 0.729 without Fc and 0.675 with Fc). Artifacts such as mass transport and crowding effects were reduced by using a low loaded H6.′TonB surface and working at high flow rate. Thus, the observed deviations from the simple model are likely due to the complexity of the FhuA·TonB interactions as suggested by the AUC results (see above).

Experiments with H6.′TonB (CT) revealed that its interaction with FhuA had an apparent lower affinity than H6.′TonB. To enhance signal response, the amount of H6.′TonB (CT) coupled to the sensor chip surface was increased to 500 RU. FhuA interacted with H6.′TonB (CT) both in the absence and presence of Fc (Fig. 2*B*). As in the case of H6.′TonB, these interactions could not be depicted by a simple model (data not shown).

Steady-state Analysis of FhuA·H6.′TonB—To examine further the interactions between FhuA and H6.′TonB and the effects of Fc, experimental conditions were changed to reach a plateau at the end of each injection. Injection times were increased to 1200 s and flow rate was decreased to 5 μl/min thereby reducing material consumption. To enhance signal response, the amount of H6.′TonB immobilized on the CM4 surface was increased to ~100 RU, and FhuA −/+ Fc injections were varied from 20 to 2000 nM. The experiments were conducted in duplicate over multiple H6.′TonB surfaces. Injections of FhuA alone demonstrated an increase in total FhuA bound to H6.′TonB compared with injections of FhuA plus Fc over the same surface (Fig. 3). Because Scatchard plots highlighted complex interactions both in the absence and presence of Fc (Fig. 3, *insets A* and *B*), the data were fit with a model assuming the presence of two distinct TonB populations displaying different affinities for FhuA. In the absence of Fc, the low affinity H6.′TonB population was determined to have an R_{max} of 166.5 RU and a K_d of 563.5 nM. The other H6.′TonB population was less abundant (R_{max} = 26.2 RU) yet displayed a higher affinity with a K_d of 36.5 nM. In the presence of Fc, the affinity related to the low affinity population was decreased by 3-fold (K_d = 1530.0 nM) and had a similar R_{max} (179.0 RU) as determined in the absence of Fc. In contrast, the affinity of FhuA for the H6.′TonB high affinity population was increased by 7-fold (K_d = 5.3 nM) in the presence of Fc and had a R_{max} of 20.0 RU similar to that determined in the absence of Fc (Table IV).

Steady-state Analysis of FhuA·H6.′TonB (CT)—To determine an apparent K_d, steady-state equilibrium analysis was conducted for H6.′TonB (CT) as previously performed for H6.′TonB. 500 RU of H6.′TonB (CT) was immobilized on the surface of a CM4 sensor chip; flow rates were set to 5 μl/min and injection times to 1200 s. FhuA −/+ Fc was injected in duplicate over multiple H6.′TonB (CT) surfaces at concentra-

tions ranging from 50 to 5600 nM. Fitting of FhuA −/+ Fc data (Fig. 4) demonstrated a single population interaction with coupled H6.′TonB (CT), suggesting a single interaction site that was confirmed by Scatchard plot analysis (Fig. 4, *insets A* and *B*). FhuA·Fc was characterized by an R_{max} of 241 RU and a K_{dapp} of 842 nM; the addition of Fc to FhuA resulted in an R_{max} of 296 RU and a K_{dapp} of 1490 nM (Table IV).

DISCUSSION

Our analytical ultracentrifugation establishes that both H6.′TonB and H6.′TonB (CT) form stable 2:1 complexes with FhuA, both in the absence and presence of ferricrocin. Although we find that H6.′TonB binds to FhuA in a 2:1 complex, the sedimentation coefficient for this complex (3.3 *s*) is significantly lower than that of FhuA plus H6.′TonB (CT) (4.5 *s*). Given the quality of the fit to our AUC data, we propose that such sedimentation behavior is well described by the non-interacting species model. SPR experiments indicate that FhuA plus H6.′TonB complex in the absence and presence of Fc is stable, as indicated by its slow dissociation (Fig. 2*A*). The sedimentation behavior of *s*3 therefore reflects a stable complex and not the reversible interactions of *s*1 (FhuA) with *s*2 (H6.′TonB) (Table II). These observations are consistent with data (Table I) that H6.′TonB alone in solution sediments anomalously (1.4 *s*) compared with H6.′TonB (CT) (1.62 *s*). Alternate conformations of H6.′TonB may contribute to multiple contacts with FhuA, including its periplasmic turns or the cork domain or the barrel wall.

In contrast to H6.′TonB (CT), we observed that in the absence of Fc, H6.′TonB is monomeric in mixtures with FhuA. This suggests that the N-terminal portion of TonB prevents homodimerization of the protein. Given that TonB is highly elongated and rigid structure (31), intramolecular interactions between the N-terminal and C-terminal portions of TonB may prevent dimerization of the C-terminal domain. We also observed a minor (<10% abundance), higher sedimenting species of TonB with a monomeric TonB molecular weight, suggesting that the protein adopts multiple conformations in solution. In the presence of Fc, however, the FhuA plus H6.′TonB mixture shows an uncomplexed H6.′TonB dimer. We propose that interaction of H6.′TonB with ligand-bound FhuA results in conformational changes in H6.′TonB that break its intramolecular interactions, allowing formation of a stable dimer. Apparently TonB dimerization is facilitated by interactions with ligand-loaded FhuA and the stable H6.′TonB retains its oligomeric state upon dissociation from FhuA.

Steady-state analysis by SPR of TonB interactions with FhuA clearly establishes that the ligand-loaded state of the OM receptor has an effect on the binding of TonB. Our analyses (Table IV) revealed two H6.′TonB populations, characterized by different affinities when binding to FhuA both in the absence and presence of Fc (Fig. 3). In contrast, binding of H6.′TonB (CT) to FhuA in the absence and presence of Fc is adequately fit as a single TonB population interacting with the OM receptor (Fig. 4). Comparing affinities determined by the steady-state analysis for binding of H6.′TonB and of H6.′TonB (CT) to FhuA, we conclude that the low affinity population detected for interaction between full-length TonB and FhuA corresponds to the binding of C-terminal TonB domain to FhuA. The additional K_d value observed for H6.′TonB demonstrates a higher affinity population. We therefore propose that these K_d values reflect a single low affinity binding region that resides in the C-terminal domain of TonB and a higher affinity binding region, which occurs outside the C-terminal domain of TonB. Affinity for FhuA may also be enhanced by a more complex set of interactions where the N-terminal binding region synergistically enhances C-terminal TonB interactions with FhuA.

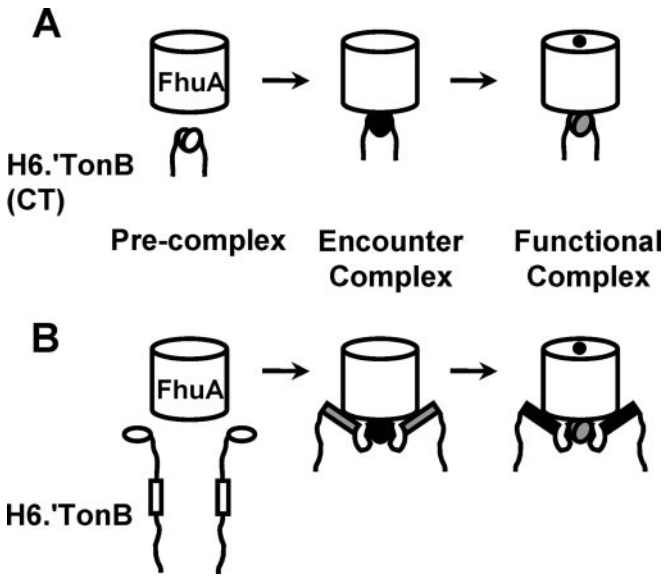

FIG. 5. **Proposed mechanisms of FhuA·TonB interactions.** The *oval shapes* represent the C-terminal domain for both H6.′TonB (CT) and H6.′TonB, whereas the *rectangular shape* represents the N-terminal domain found in H6.′TonB only. *Differences in shading* represent the modulations in affinity caused by Fc. *Dark gray* shading indicates a strong affinity, whereas *light gray* depicts a weak affinity. *Panel A* represents the interaction between the H6.′TonB (CT) protein and FhuA. The pre-complex consists of detergent-solubilized FhuA and dimerized H6.′TonB (CT). An encounter complex forms prior to the addition of Fc in which the H6.′TonB (CT) dimer binds to FhuA. Upon addition of Fc, the affinity of interaction of the H6.′TonB (CT) dimer for FhuA is reduced to form a functional complex. *Panel B* depicts the interactions between H6.′TonB and FhuA. The pre-complex involves two H6.′TonB monomers and FhuA. Transition to the encounter complex involves binding to FhuA at both the N-terminal and C-terminal domains of each H6.′TonB monomer, yielding a bound dimer of H6.′TonB. Upon addition of Fc, the affinity of the N-terminal domain of TonB for FhuA increases; the affinity of the C-terminal domain decreases.

SPR experiments show that the low affinity binding region and the high affinity binding region respond to the addition of Fc in an inverse manner (Table IV). Whereas the K_d for the low affinity binding region observed in experiments with both H6.′TonB and H6.′TonB (CT) increases ~2-fold in the presence of Fc, the K_d for the high affinity binding region in H6.′TonB decreases about 7-fold in the presence of ligand. Our AUC results support this observation, because in the presence of Fc almost all FhuA is complexed to H6.′TonB. In contrast, even in the presence of excess H6.′TonB (CT) and Fc, a significant population of uncomplexed FhuA remains in mixtures of FhuA and H6.′TonB (CT). This may reflect conformational rearrangements occurring at the high affinity binding region upon ligand loading of the OM receptor, resulting in the large change in K_d observed in the SPR experiments. Taken together, these results provide the first evidence that a FhuA-binding region on TonB exists outside the C-terminal domain of TonB. This high affinity binding region is more sensitive to the ligand-loaded state of the OM receptor than the low affinity binding region, which corresponds to the C-terminal domain. We propose that TonB associates with FhuA in two discrete states: a complex that reflects transient encounters and a more stable functional complex, which is necessary for TonB-dependent energy transduction. The Fc-independent encounter complex is not equivalent to the functional complex that involves a modulation of affinities within the two binding regions.

Interaction models for H6.′TonB (CT) and H6.′TonB with FhuA are illustrated in Fig. 5. Our analyses indicate that the C-terminal domain of TonB exists in solution as a dimer and it

forms an encounter complex with FhuA even in the absence of Fc. The affinity of interaction decreases when FhuA is loaded with Fc. Therefore, interactions between FhuA and the C-terminal domain of TonB are stronger when the OM receptor is in a ligand-free state. Upon binding of ligand, the affinity of H6.′TonB (CT) for FhuA decreases; however, they remain complexed (Fig. 5*A*). The solution state of H6.′TonB has been shown to be monomeric, indicating that complexation of H6.′TonB and FhuA is initiated by a single H6.′TonB. Dimerization of TonB may then be facilitated by interactions involving two bound TonB monomers with the OM receptor. Of the two affinities determined for H6.′TonB by SPR analyses, the lower affinity corresponds well to the C-terminal portion of the protein; the higher affinity region resides N-terminal to residue 154. In the absence of Fc, both binding regions interact with FhuA with their affinities specified in Table IV. Upon binding of ligand to FhuA, binding at the low affinity site decreases with a concomitant increase in affinity at the high affinity site in the N-terminal portion of TonB, thereby facilitating transition to the functional complex (Fig. 5*B*).

In the context of TonB-OM receptor interactions, the models of binding proposed in Fig. 5 can be expanded to incorporate known structural changes caused by Fc. The unwinding of the switch helix and the translocation of the N terminus of FhuA upon Fc binding, as resolved by x-ray crystallography (6), may result in the decreased affinity observed at the C-terminal binding region. This large conformational change in FhuA may also allow for the Fc-induced enhancement of binding at the higher affinity region. To date, it has been recognized that TonB-OM receptor interactions are enhanced upon ligand binding, but not at a site other than the C terminus, and it is now evident that other sites within TonB are also critical.

Our proposed models are consistent with certain aspects of the "shuttle model" of TonB interaction with OM receptors proposed by Postle and Kadner (19). In this model, TonB is proposed to make initial contact with the OM receptor through its C-terminal domain. This contact results in dissociation of TonB from the ExbB·ExbD complex enabling additional contacts between the OM receptor and sites within the N-terminal domain of TonB. Indeed, our SPR data support this model in that we show potential contacts between the N terminus of TonB and FhuA. Our data also support aspects of the "propeller model" proposed by Chang *et al.* (18) in which dimerization of TonB is necessary for complexation with the OM receptor such that energy-dependent ligand transfer can occur. This is consistent with our concept of a functional TonB·FhuA complex.

Recently, *in vivo* dimerization studies of TonB demonstrated (32) that TonB (residues 164–239) fused to the cytoplasmic ToxR (residues 1–182) has a strong propensity to form dimers in the periplasm. This observation matches our AUC results for H6.′TonB (CT) dimerization. Their study also demonstrated that TonB (residues 33–239) fused to cytoplasmic ToxR did not dimerize, a result substantiated by AUC analysis of H6.′TonB. Sauter *et al.* proposed that interactions of TonB with the ligand-loaded OM receptor FecA may affect TonB dimerization, consistent with our observations. The *in vivo* dimerization study, taken together with our results, reconcile aspects of the shuttle and propeller models and suggest that more intricate mechanisms of TonB interactions with OM receptors must be considered.

Acknowledgments—We thank M. O'Connor-McCourt and P. Schuck for insightful comments in preparation of the manuscript and J.-N. Gagnon for critical reading. AUC support was from J.-C. Lavoie and L. Knafo, Montreal and from colleagues at the 2002 Workshop on Analytical Ultracentrifugation, University of Connecticut, Storrs, CT. Sheldon Biotechnology Center is supported by a Multi-user Maintenance Grant from CIHR.

REFERENCES

1. Braun, V., Hantke, K., and Köster, W. (1998) in *Metal Ions in Biological Systems* (Sigel, A., and Sigel, H., eds) Vol. 35, pp. 67–145, Marcel Dekker, Inc., New York
2. Moeck, G. S. , and Coulton, J. W. (1998) *Mol. Microbiol.* **28,** 675–681
3. Ferguson, A. D., Coulton, J. W., Diederichs, K., and Welte, W. (2001) in *Handbook of Metalloproteins*in (Messerschmidt, A., Huber, R., Poulos T., and Wieghardt, K., eds) pp. 834–849, John Wiley & Sons, Ltd., Chichester
4. Braun, V., and Braun, M. (2002) *Curr. Opin. Microbiol.* **5,** 194–201
5. Moeck, G. S. , Tawa, P., Xiang, H., Ismail, A. A., Turnbull, J. L., and Coulton, J. W. (1996) *Mol. Microbiol.* **22,** 459–471
6. Ferguson, A. D., Hofmann, E., Coulton, J. W., Diederichs, K., and Welte, W. (1998) *Science* **282,** 2215–2220
7. Locher, K. P., Rees, B., Koebnik, R., Mitschler, A., Moulinier, L., Rosenbusch, J. P., and Moras, D. (1998) *Cell* **95,** 771–778
8. Ferguson, A. D., Chakraborty, R., Smith, B. *s.* , Esser, L., van der Helm, D., and Deisenhofer, J. (2002) *Science* **295,** 1715–1719
9. Buchanan, S. K., Smith, B. S. , Venkatramani, L., Xia, D., Esser, L., Palnitkar, M., Chakraborty, R., van der Helm, D., and Deisenhofer, J. (1999) *Nat. Struct. Biol.* **6,** 56–63
10. Chimento, D. P., Kadner, R. J., and Wiener, M. C. (2003) *J. Mol. Biol.* **332,** 999–1014
11. Skare, J. T., Ahmer, B. M., Seachord, C. L., Darveau, R. P., and Postle, K. (1993) *J. Biol. Chem.* **268,** 16302–16308
12. Schoffler, H., and Braun, V. (1989) *Mol. Gen. Genet.* **217,** 378–383
13. Gunter, K., and Braun, V. (1990) *FEBS Lett.* **274,** 85–88
14. Moeck, G. S., Coulton, J. W., and Postle, K. (1997) *J. Biol. Chem.* **272,** 28391–28397
15. Moeck, G. S., and Letellier, L. (2001) *J. Bacteriol.* **183,** 2755–2764
16. Cadieux, N., and Kadner, R. J. (1999) *Proc. Natl. Acad. Sci. U. S. A.* **96,** 10673–10678
17. Cadieux, N., Bradbeer, C., and Kadner, R. J. (2000) *J. Bacteriol.* **182,** 5954–5961
18. Chang, C., Mooser, A., Pluckthun, A., and Wlodawer, A. (2001) *J. Biol. Chem.* **276,** 27535–27540
19. Postle, K., and Kadner, R. J. (2003) *Mol. Microbiol.* **49,** 869–882
20. Zhai, Y. F., Heijne, W., and Saier, M. H., Jr. (2003) *Biochim. Biophys. Acta* **1614,** 201–210
21. Larsen, R. A., Letain, T. E., and Postle, K. (2003) *Mol. Microbiol.* **49,** 211–218
22. Ferguson, A. D., Breed, J., Diederichs, K., Welte, W., and Coulton, J. W. (1998) *Protein Sci.* **7,** 1636–1638
23. Schuck, P. (2000) *Biophys. J.* **78,** 1606–1619
24. Johnsson, B., Lofas, S., and Lindquist, G. (1991) *Anal. Biochem.* **198,** 268–277
25. Rich, R. L., and Myszka, D. G. (2000) *Curr. Opin. Biotechnol.* **11,** 54–61
26. De Crescenzo, G., Grothe, S., Lortie, R., Debanne, M. T., and O'Connor-McCourt, M. (2000) *Biochemistry* **39,** 9466–9476
27. De Crescenzo, G., Grothe, S., Zwaagstra, J., Tsang, M., and O'Connor-McCourt, M. D. (2001) *J. Biol. Chem.* **276,** 29632–29643
28. Boulanger, P., le Maire, M., Bonhivers, M., Dubois, S., Desmadril, M., and Letellier, L. (1996) *Biochemistry* **35,** 14216–14224
29. Perkins, S. J. (1986) *Eur. J. Biochem.* **157,** 169–180
30. Chimento, D. P., Mohanty, A. K., Kadner, R. J., and Wiener, M. C. (2003) *Nat. Struct. Biol.* **10,** 394–401
31. Evans, J. S., Levine, B. A., Trayer, I. P., Dorman, C. J., and Higgins, C. F. (1986) *FEBS Lett.* **208,** 211–216
32. Sauter, A., Howard, S. P., and Braun, V. (2003) *J. Bacteriol.* **185,** 5747–5754